Moisture Effect on the Response of Orthotropic Stiffened Panel Structures

Constantinos S. Lyrintzis*
San Diego State University, San Diego, California
and
Dimitri A. Bofiliost
Integrated Aerospace Sciences Corporation, San Diego, California and Athens, Greece

This paper examines the effect of absorbed moisture on the dynamic response of stiffened panel structure from orthotropic material and a general external loading condition. An analysis of orthogonally anisotropic stiffened plates subject to loads induced by the moisture and random external pressure is presented. The procedure is based on the linear theory of plates and beams utilizing modified transfer matrices to accommodate the effect of the moisture. Ingestion of moisture was taken to vary linearly with the swelling which results in effective force resultants. Numerical results indicative of the moisture effect are offered.

Introduction

AEROSPACE structures, aircraft, and other transportation vehicles are composed of flat or curved panels. The panels usually have length-wise stiffeners. Vibrations induced by various sources such as thrusters, mechanical and electrical equipment, exhaust noise, turbulent boundary layer flow, oscillating shocks, jet noise, etc., could have a direct effect on the quality and limitation of the precision requirements and comfort levels inside the aerospace structures. Thus, there is a need for accurate and precise solutions.[1-3]

Approximate and numerical solutions for the vibration response of the surface protection systems of the aircraft utilize the finite-element methods. These solutions require large computer storage capabilities, and when the vibrations are coupled to the acoustic field, the results are limited to very low frequencies.[3] Analytical solutions for the dynamic response to aircraft panels have also been developed. Analytical models are usually limited to simplified geometries and do not include geometric details, but the solution is given in compact form, and the computed time required is limited. An analytical approach for an aluminum and composite shell is presented in Refs. 4 and 5. These models did not account for the discrete stiffening effect. Analytical solutions for dynamic response of discretely stiffened panels from homogeneous isotropic[6-10] and composite[11] materials have been developed. However, in all the previous approaches, the hygrothermal effect is not present. Investigations have shown the deleterious effects of hygrothermal environments of structural performance of nonisotropic materials.[12-16] The deleterious effects consist of degradation of the mechanical properties and hygroscopic expansions.[13] The hygrothermal effects are two. One is associated with the temperature, and the second with the moisture ingestion. At any temperature there is a shift in the stiffness and strength curves. These curves are lowered by the absorbed moisture.[12] Because of the swelling, significant residual stresses are induced by moisture absorption.[15] Ingestion of moisture has an effect similar to the thermal effect.[12-15]

Received Aug. 10, 1989; revision received Nov. 29, 1989.

*Assistant Professor, Department of Aerospace Engineering and Engineering Mechanics. Member AIAA.

†Technical Director, Department of Research and Development. Member AIAA.

This paper examines the effect of absorbed moisture (only one of the hygrothermal effects) on the dynamic response of stiffened panel structure from orthotropic materials. Figure 1 illustrates a typical stiffened panel structure. A transfer matrix procedure has been developed to include the orthotropy of the material and the moisture effect (coefficients of hygrothermal expansion) for plates with stiffeners due to general external loading condition. It is taken that the ingestion of moisture varies linearly with the swelling. Details for the coupling of the stiffeners and the plates are offered. Numerical results indicative of the moisture effect are also presented.

Response of an Orthotropic Panel

Consider a thin flat plate. The material of the plate has three planes of symmetry with respect to its elastic properties. This material (orthotropic or orthogonally anisotropic) covers a lot of cases of composite materials and is mostly used to bring the theory into agreement with experiments. Taking the symmetry planes as coordinate planes, the relations between the stress and strain components can be represented by the following equations:

$$\sigma_x = \frac{E_x}{\nu_{00}}(\varepsilon_x - \beta_x \Delta M_0) + \frac{\nu_{xy}E_y}{\nu_{00}}(\varepsilon_y - \beta_y \Delta M_0) \tag{1}$$

$$\sigma_y = \frac{\nu_{xy}E_y}{\nu_{00}}(\varepsilon_x - \beta_x \Delta M_0) + \frac{E_y}{\nu_{00}}(\varepsilon_y - \beta_y \Delta M_0) \tag{2}$$

$$\sigma_{xy} = G\gamma_{xy} \tag{3}$$

where E_i are the elastic modulus, β_i are the coefficients of hygroscopic expansion, ΔM_0 is the change in moisture concentration function (wt%). Also, ν_{xy} is the Poisson ratio (i.e., the negative of the ratio of the strain in y direction to the strain in the x direction due to an applied stress in the x direction). Thus, $\nu_{xy}E_y = \nu_{yx}E_x$.
Also,

$$\nu_{00} = 1 - \nu_{xy}\nu_{yx} \tag{4}$$

The relations of Eqs. (1-3) require that hygroscopic deformations are accurately described by linear coefficients of hygroscopic expansion.[12-15] We note that hygrothermal effects are dilitational only, that is, they cause an expansion or contraction, but do not affect the shear stresses or strains. We are interested in the dynamic aspect of the problem. However, if we assume that moisture effects have operated for a long

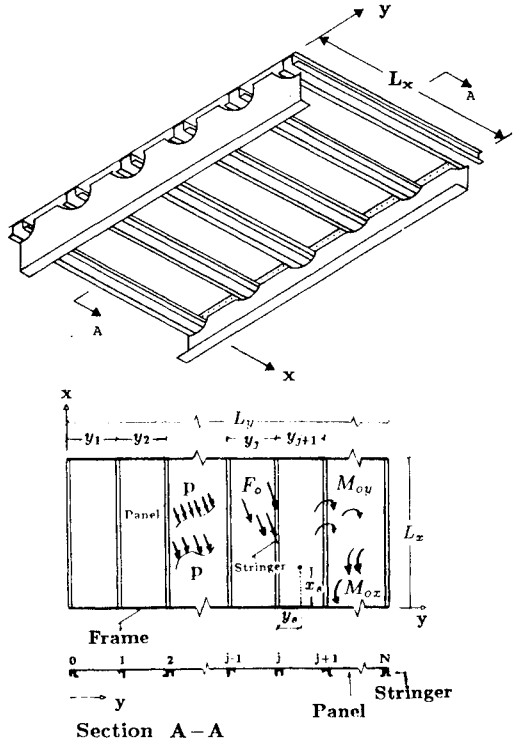

Fig. 1 Stiffened multispanned panel array.

period of time, then, ΔM_0 will not be a function of time, but only a function of the spatial coordinate z (quasistatic).

Using the constitutive equations, the hygrothermal contribution can be determined. The integrated hygrothermal stress resultants are given by

$$N_x^m = \frac{E_x\beta_x + \nu_{xy}E_y\beta_y}{\nu_{00}} \int_{-h/2}^{h/2} \Delta M_0 \, dz \tag{5}$$

$$N_y^m = \frac{\nu_{xy}E_y\beta_x + E_y\beta_y}{\nu_{00}} \int_{-h/2}^{h/2} \Delta M_0 \, dz \tag{6}$$

$$N_{xy}^m = 0 \tag{7}$$

where h is the thickness of the orthotropic plate, and the superscript m indicates the dependance on the moisture concentration. Similarly, for the flexural response, it is necessary to define the effective moment resultants:

$$M_x^m = \frac{E_x\beta_x + \nu_{xy}E_y\beta_y}{\nu_{00}} \int_{-h/2}^{h/2} \Delta M_0 z \, dz \tag{8}$$

$$M_y^m = \frac{\nu_{xy}E_y\beta_x + E_y\beta_y}{\nu_{00}} \int_{-h/2}^{h/2} \Delta M_0 z \, dz \tag{9}$$

$$M_{xy}^m = 0 \tag{10}$$

In addition to hygrothermal loads, the panels are subjected to mechanical external loads, such as random pressure, point forces, and point couples. The stiffened panel shown in Fig. 1 located at $z = 0$, $0 \leqslant x \leqslant L_x$, $0 \leqslant y \leqslant L_y$ is simply supported at the edges normal to the stiffeners. Using classical thin-plate theory, the equation of motion governing the bending vibrations of a panel from orthotropic material located between any two arbitrary stiffeners is[8,9,17–19]

$$\frac{h^3}{12}\left[\frac{E_x}{\nu_{00}} w_{,xxxx} + 2\left(\frac{\nu_{xy}E_y}{\nu_{00}} + 2G_{xy}\right) w_{,xxyy} + \frac{E_y}{\nu_{00}} w_{,yyyy}\right] + c\dot{w}$$
$$+(1 + 0.01\Delta M_0)\rho h\ddot{w} = p^{ex} - p^m$$
$$+N_x w_{,xx} + 2N_{xy} w_{,xy} + N_y w_{,yy} \tag{11}$$

where a comma denotes a derivative and $w(x,y,t)$ is the normal deflection, c is the viscous damping coefficient, and ρ is the panel mass density. The factor $(1 + 0.01\Delta M_0)$ in front of the mass of the system accounts for the absorbed moisture. In Eq. (11) we note that the loads on the panel are the mechanical external pressure p^{ex}, the pressure because of the hygroscopic moments p^m, and the stress resultants N_x, N_y, N_{xy}. More specifically, the mechanical loads p^{ex} consist of external random pressure $p^r(x,y,t)$, and N_f number of random point loads F_i located at (x_i,y_i), and N_{M_x}, N_{M_y} number of random point couples M_{ix}, M_{iy} acting on a plane parallel to x and y, respectively, located at (x_i,y_i). Thus,

$$p^{ex} = p^r(x,y,t) + \sum_{i=1}^{N_f} F_i(t)\delta(x - x_i)\delta(y - y_i)$$
$$+ \sum_{i=1}^{N_{My}} M_{iy}(t)\delta(x - x_i)\delta_{,y}(y - y_i)$$
$$+ \sum_{i=1}^{N_{Mx}} M_{ix}(t)\delta_{,x}(x - x_i)\delta(y - y_i) \tag{12}$$

where δ is the Dirac delta function, and a comma denotes a derivative. Also the pressure because of the hygroscopic moments is[17,19]

$$p^m = M_{x,xx}^m + M_{y,yy}^m \tag{13}$$

where M_x^m and M_y^m are given in Eqs. (8) and (9). When moisture and temperature concentration distributions are not functions of x and y, it is $p^m = 0$. Also in Eq. (10) the stress resultants can be found to be

$$N_x = \frac{h}{\nu_{00}}(E_x u_{,x} + \nu_{xy}E_y v_{,y}) - N_x^m \tag{14}$$

$$N_y = \frac{h}{\nu_{00}}(\nu_{xy}E_y u_{,x} + E_y v_{,y}) - N_y^m \tag{15}$$

$$N_{xy} = hG_{xy}(u_{,y} + v_{,x}) \tag{16}$$

where u,v are the in-plane displacements in the x,y direction, respectively. The N_x^m and N_y^m are given in Eqs. (5) and (6).

Taking the in-plane displacements $u = v = 0$ (panel restrained along the edges) in Eqs. (14–16), and using that $p^m = 0$ (moisture distributions not functions of x and y), Eq. (11) results in a simpler form. The differential equation now has only even derivatives of the unknowns.

The panel displacement w can be expressed in terms of the expansion

$$w(x,y,t) = \sum_{n=1}^{\infty} q_n(y,t)X_n(x) \tag{17}$$

where q_n are the generalized coordinates and X_n are the normal modes corresponding to the x direction. The terms X_n depend on the boundary conditions at $x = 0$ and $x = L_x$. These terms are the modes of a beam with length L_x and the same boundary conditions as the panel at $x = 0, L_x$ at its ends. Thus, for the simplest case of simple supports at the edges normal to the stiffeners, $X_n = \sin(n\pi x/L_x)$.

Assuming that all loads have operated for a long period of time, we can solve the differential equation in the frequency domain. Taking Fourier transformation of Eqs. (11–17) and following the Galerkin procedure, Eq. (11) reduces to

$$\bar{q}_{n,yyyy} - 2K_1\bar{q}_{n,yy} + K_2\bar{q}_n = Q_n \tag{18}$$

where the overbar denotes the Fourier transform of the

quantity and

$$K_1 = \left(\frac{n\pi}{L_x}\right)^2 \frac{v_{xy}E_y + 2v_{00}G_{xy}}{E_y} - \frac{6v_{00}A_y^m}{E_y h^3} \tag{19}$$

$$K_2 = \left(\frac{n\pi}{L_x}\right)^4 \frac{E_x}{E_y} + \frac{12v_{00}(i\omega - \rho h\omega^2)}{E_y h^3} - \left(\frac{n\pi}{L_x}\right)^2 \frac{12v_{00}A_x^m}{E_y h^3} \tag{20}$$

in which $i = \sqrt{-1}$, and

$$A_x^m = \frac{\Delta M_0 h}{v_{00}}[E_x\beta_x + v_{xy}E_y\beta_y] \tag{21}$$

$$A_y^m = \frac{\Delta M_0 h}{v_{00}}[v_{xy}E_y\beta_x + E_y\beta_y] \tag{22}$$

Also, in Eq. (18) the generalized forces Q_n are

$$Q_n(y,\omega) = \frac{24v_{00}}{E_y h^3 L_x}\left[\int_0^{L_x} \bar{p}^r(x,y,\omega)X_n(x)\,dx + \sum_{i=1}^{N_f} \bar{F}_i(\omega)X_n(x_i)\delta(y-y_i) + \sum_{i=1}^{N_{M_y}} \bar{M}_{iy}(\omega)X_n(x_i)\delta_{,y}(y-y_i) + \sum_{i=1}^{N_{M_x}} \bar{M}_{ix}(\omega)X_{n,x}(x_i)\delta(y-y_i)\right] \tag{23}$$

The roots of the characteristic equation resulting from Eq. (18) are $\pm\sigma_{1n}$, $\pm i\sigma_{2n}$, where

$$\sigma_{1n,2n} = (\sqrt{K_1^2 - K_2} \pm K_1)^{1/2} \tag{24}$$

The solution of Eq. (18) can be written as a superposition of homogeneous and particular solutions

$$\bar{q}_n = \bar{q}_n^h + \bar{q}_n^p \tag{25}$$

The homogeneous solution can be written as

$$\bar{q}_n^h(y,\omega) = \sum_{i=0}^{3} C_{in}f_{in}(y) \tag{26}$$

where C_{in} are arbitrary constants to be determined from the boundary conditions, and functions $f_{in}(y)$ are given in Refs. 6 and 7. The arbitrary constants can be expressed in terms of q_n and $q_{n,y}$ and $q_{n,yy}$ and $q_{n,yyy}$ evaluated at the boundary $y = 0$. The particular solution can be obtained by first taking the Laplace transform of Eq. (18) with respect to y and then obtaining the inverse solution (as in Ref. 7). Thus,

$$\bar{q}_n(y,\omega) = \sum_{i=0}^{3} C_{in}f_{in}(y) + \int_0^y f_{3n}(y-\xi)Q_n(\xi,\omega)\,d\xi \tag{27}$$

Differentiating Eq. (27) and introducing the relationships between various derivatives of $\bar{q}_n(y,\omega)$ in terms of slope, bending moment, and shear, the response of an orthotropic panel can be written in a convenient state vector form[6-10]

$$\{Z_n\} = \{\delta_n,\theta_n,M_n,V_n\}^T \tag{28}$$

where the superscript ^{T} denotes the transpose of a matrix and $\delta_n,\theta_n,M_n,V_n$ are modal components of deflection, slope, moment, and shear, respectively. Then, the response state vector at station j on the panel is[9]

$$\{Z_n\}_j^l = [F]_j\{Z_n\}_{j-1}^r + \int_0^{y_j} [F(y_j-\xi)]\{P_n(\xi)\}\,d\xi \tag{29}$$

where the superscripts l and r indicate either the left or right side of station j, respectively, and $\{P_n(\xi)\}$ is the matrix of generalized random forces

$$\{P_n(\xi)\} = \{0,0,0,E_y h^3 Q_n/(12v_{00})\}^T \tag{30}$$

Also, $[F]$ is the field transfer matrix which transfers the state vector across the orthotropic panel[6-8]

$$[F]_j = [B]_j[R]_j[B]_j^{-1} \tag{31}$$

with matrices $[R]$ having the same form as that given in Refs. 6 and 7, but now the charcteristic roots from Eq. (24) have to be used. Also the new form of matrices $[B]$ and $[B]^{-1}$ can be found to be

$$[B] = \begin{bmatrix} 1 & 0 & 0 & 0 \\ 0 & 1 & 0 & 0 \\ -\dfrac{v_{xy}E_y h^3}{12v_{00}}\left(\dfrac{n\pi}{L_x}\right)^2 & 0 & \dfrac{E_y h^3}{12v_{00}} & 0 \\ 0 & -\dfrac{h^3}{12}\left(\dfrac{v_{xy}E_y}{v_{00}} + 4G_{xy}\right)\left(\dfrac{n\pi}{L_x}\right)^2 & 0 & \dfrac{E_y h^3}{12v_{00}} \end{bmatrix} \tag{32}$$

and

$$[B]^{-1} = \begin{bmatrix} 1 & 0 & 0 & 0 \\ 0 & 1 & 0 & 0 \\ v_{xy}\left(\dfrac{n\pi}{L_x}\right)^2 & 0 & \dfrac{12v_{00}}{E_y h^3} & 0 \\ 0 & \left(v_{xy} + 4v_{00}\dfrac{G_{xy}}{E_y}\right)\left(\dfrac{n\pi}{L_x}\right)^2 & 0 & \dfrac{12v_{00}}{E_y h^3} \end{bmatrix} \tag{33}$$

Effect of the Stiffeners

To transfer a state vector across the stiffeners, point transfer matrices to account for the interaction between the stiffeners and the panels need to be developed. In addition to bending and twisting, hygrothermal effects are induced. The stiffeners used in aerospace structures are usually thin-walled members with an open shape cross section as shown in Figs. 1 and 2. The point of connection between the skin and the stiffener is assumed to be at the horizontal projection of the shear center (see Fig. 2). The stiffener does not have any effect on the continuity of the deflections and the slopes in the skin on either side of the line of the attachment.[6-9] Thus,

$$\{\bar{q}_n\}_j^r = \{\bar{q}_n\}_j^l \tag{34}$$

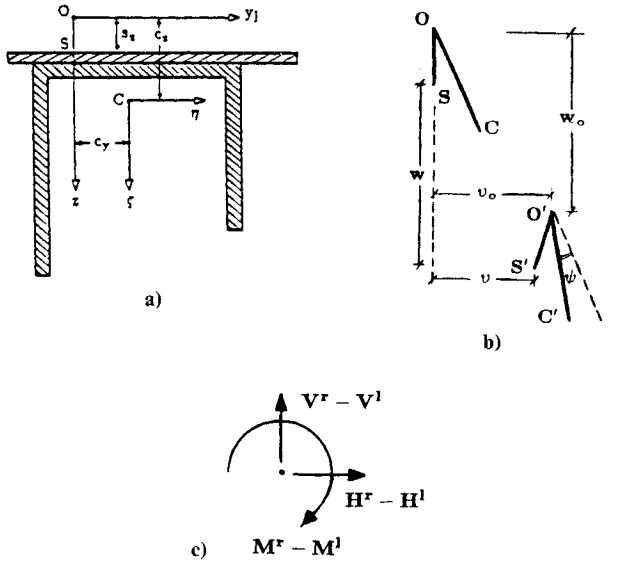

Fig. 2 A typical stiffener: a) cross section; b) displacements; c) forces and moment transferred to the stiffener from the skin.

$$\{\bar{q}_{n,y}\}_j^r = \{\bar{q}_{n,y}\}_j^l \tag{35}$$

However, when the panels vibrate, the elastic stiffeners also vibrate, and changes in the moment and shear components of the state vector occur. The equations governing the deflections of the stiffener (beam) were established at the beginning of the century.[17,19] These equations can be modified to fit the transfer matrix formulation[6,7,9] and now include the moisture expansion

$$E_s I_\eta w_{0,xxxx} + E_s I_{\eta\zeta} v_{0,xxxx} + P^m w_{c,xx} + M^m_{s\eta,xx} = \underline{p}(x) \tag{36}$$

$$E_s I_\zeta v_{0,xxxx} + E_s I_{\eta\zeta} w_{0,xxxx} + P^m v_{c,xx} + M^m_{s\zeta,xx} = \underline{q}(x) \tag{37}$$

$$E_s C_w \psi_{,xxxx} - \left(\int_A \sigma^m_{sx} r^2 \, dA + G_s C_s\right)\psi_{,xx} = \underline{r}(x) \tag{38}$$

where the comma denotes again differentiation; v and w are normal to the stiffeners and vertical displacements, respectively; the subscripts 0 and c refer the deflections with respect to the shear center and center of gravity, respectively; ψ is the angular rotation of the stiffeners; E_s and G_s are the moduli of elasticity of the stiffener; $I_\eta, I_\zeta, I_{\eta\zeta}$ are the centroidal moments of inertia and product moment of inertia; C_w is the warping constant of the cross section with respect to the shear center; C_s is the Saint-Venant constant of uniform torsion; r is the distance from the shear center; and A the cross-sectional area. Also, P^m, $M^m_{s\eta}$, and $M^m_{s\zeta}$ depend on the moisture concentration:

$$P^m = \int_A E_s \beta_s \Delta M_0 \, dA \tag{39}$$

$$M^m_{s\eta} = \int_A E_s \beta_s \Delta M_0 \eta \, dA \tag{40}$$

$$M^m_{s\zeta} = \int_A E_s \beta_s \Delta M_0 \zeta \, dA \tag{41}$$

The portion of the stress due to the moisture alone is

$$\sigma^m_{sx} = -E_s \beta_s \Delta M_0 + \frac{P^m}{A} + \left(\frac{I_\eta M^m_{s\zeta} - I_{\eta\zeta} M^m_\eta}{I_\eta I_\zeta - I^2_{\eta\zeta}}\right)\eta + \left(\frac{I_\zeta M^m_{s\eta} - I_{\eta\zeta} M^m_\zeta}{I_\eta I_\zeta - I^2_{\eta\zeta}}\right)\zeta \tag{42}$$

with β_s the hygroscopic coefficient of the stiffener, and (η,ζ) a centroidal coordinate system (see Fig. 2). Usually the moisture concentration ΔM_0 is not a function of x, then $M^m_{s\eta,xx} = 0 = M^m_{s\zeta,xx}$. We note that $\sigma^m_{sx} = 0$ only at the very special case when the cross section of the stiffener is doubly symmetrical and then $M^m_{s\eta} = 0 = M^m_{s\zeta}$. At all of the other cases $\sigma^m_{sx} \neq 0$.

In Eqs. (36–38) $\underline{p}$ and $\underline{q}$ are the distributed loads at the shear center along the stiffener, acting in the z and y directions, respectively; $\underline{r}$ is the distributed torque about the shear center. Because of the elastic deformation of the stiffener, vertical and horizontal forces and torque can be summed through shear center O (see Fig. 2). The inertia forces are more conveniently summed about the centroid C. In addition, there are forces and moments transmitted from the panels at the point of the attachment S. Thus the distributed loads are[6,7,20]

$$\underline{p}(x) = (-V^r + V^l) - \rho^m_s A \ddot{w}_c \tag{43}$$

$$\underline{q}(x) = (H^r - H^l) - \rho^m_s A \ddot{v}_c \tag{44}$$

$$\underline{r}(x) = (M^r - M^l) - (N^r - N^l)s_z + \rho^m_s A \ddot{v}_c c_z - \rho^m_s \ddot{w}_c c_y - \rho^m_s J_c \ddot{\psi} \tag{45}$$

in which ρ^m_s, the density of the stiffener, is

$$\rho^m_s = (1 + 0.01\,\Delta M_0)\rho_s \tag{46}$$

where ρ_s is the mass density; $V^{r,l}$, $H^{r,l}$, and $M^{r,l}$ are the vertical, horizontal forces, and moment, respectively, transmitted from the panel at the right or left of the stiffener; J_c is the polar moment of inertia with respect to the centroid; and s_z, c_z, c_y are distances defined in Fig. 2. The deflections of the stiffener at the point of the attachment S (denoted as w,v with no subscript) are geometrically related to those at the centroid (w_c, v_c) and shear center (w_0, v_0) as follows[6,20]:

$$w = w_0 - s_z(1 - \cos\psi) \approx w_0 \tag{47}$$

$$v = v_0 - s_z\psi \tag{48}$$

$$w_c = w_0 + c_y\psi \tag{49}$$

$$v_c = v_0 - c_z\psi \tag{50}$$

Substituting Eqs. (47–50) into the equations of motion, Eqs. (36–38), and using Eqs. (43–45), expressions for $(M^r - M^l)$, $(V^r - V^l)$, and $(H^r - H^l)$, as functions of the displacements w,v,ψ (at the shear center), can be obtained. The expression for $M^r - M^l$ will involve the horizontal forces $H^r - H^l$, but these can be eliminated by using the third obtained expression. Thus, finally, the expressions for $(M^r - M^l)$ and $(V^r - V^l)$ are only functions of displacements, the inertia forces, and the geometric characteristics of the stiffener. Recognizing the rigidity of the structure in the plane of the skin, the lateral motions can be neglected, i.e., $v = 0$ and $v_c = (s_z - c_z)\psi$. Furthermore, the in-plane forces induced by bending and by side sway from $H^r - H^l$ have a negligible effect on the plate motion.[6,7] Substituting $v = 0$, $\partial w/\partial y = \psi$, and the mode expansion equation (17) for displacement w, into the expressions for $(M^r - M^l)$ and $(V^r - V^l)$, and using orthogonality condition, it can be shown that

$$M^r_n - M^l_n = \hat{b}_n \delta_n + \hat{c}_n \theta^n \tag{51}$$

$$V^r_n - V^l_n = -\hat{e}_n \delta_n - \hat{d}_n \theta_n \tag{52}$$

where δ_n, θ_n are modal components of the state vector defined in Eq. (28). Also, $\hat{b}_n, \hat{c}_n, \hat{e}_n, \hat{d}_n$ are functions of the frequency

and depend on index n:

$$\hat{b}_n(\omega) = E_s I_{\eta\zeta} s_z \left(\frac{n\pi}{L_x}\right)^4 - \omega^2 \rho_s^m A c_y \tag{53}$$

$$\hat{c}_n(\omega) = E_s C_{ws} \left(\frac{n\pi}{L_x}\right)^4 - \omega^2 \rho_s^m J_s + \left[G_s C_s + P^m s_z (c_z - s_z) + \int_A \sigma_{sx}^m r^2 \, dA\right] \left(\frac{n\pi}{L_x}\right)^2 \tag{54}$$

$$\hat{e}_n(\omega) = E_s I_\eta \left(\frac{n\pi}{L_x}\right)^4 - \omega^2 \rho_s^m A - P^m \left(\frac{n\pi}{L_x}\right)^2 \tag{55}$$

$$\hat{d}_n(\omega) = E_s I_{\eta\zeta} s_z \left(\frac{n\pi}{L_x}\right)^4 - \omega^2 \rho_s^m A c_y - P^m c_y \left(\frac{n\pi}{L_x}\right)^2 \tag{56}$$

in which

$$J_s = J_c + A c_y^2 + A(c_z - s_z)^2 \tag{57}$$

the equivalent warping constant of the stiffener cross section with respect to point of connection S as the center of twist is

$$C_{ws} = C_w + I_\zeta s_z^2 \tag{58}$$

From Eqs. (34), (35), (51), and (52), the state vector across the stiffening element at station j can be expressed as

$$\{Z_n\}_j^r = [G]_j \{Z_n\}_j^l \tag{59}$$

where

$$[G]_j = \begin{bmatrix} 1 & 0 & 0 & 0 \\ 0 & 1 & 0 & 0 \\ \hat{b}_n & \hat{c}_n & 1 & 0 \\ -\hat{e}_n & -\hat{d}_n & 0 & 1 \end{bmatrix} \tag{60}$$

and where $[G]_j$ is the point transfer matrix associated with the physical constants of the jth stiffener.

Response of the Stiffened Panel

Using Eqs. (29) and (59), the state vector for a multibay orthotropic panel shown in Fig. 1 can be expressed at any arbitrary locations s, where $s = y_s + \Sigma_{m=1}^{j} y_m$, as[8,9]

$$\{Z_n\}_s^l = {}_s^l[T]_0^l \{Z_n\}_0^l + {}_s^l\{E_n\}_0^l \tag{61}$$

where matrix ${}_s^l[T]_0^l$ transfers the state vector from station 0 to station s such that

$${}_s^l[T]_0^l = [F_s][G]_j[F]_j[G]_{j-1} \cdots [F]_1[G]_0 \tag{62}$$

in which $[F_s]$ is a field transfer matrix which transfers the state vector over a portion of a panel located between stations j and $j+1$. Transfer matrix ${}_s^l\{E_n\}_0^l$ represents the effect of distributed and concentrated loads[7,8]

$${}_s^l\{E_n\}_0^l = {}_s^l[T]_1^l \{L_{1n}\} + {}_s^l[T]_2^l \{L_{2n}\} + \cdots + {}_s^l[T]_j^l \{L_{jn}\} + \{L_{sn}\} \tag{63}$$

where

$$\{L_{jn}\} = \int_0^{y_j} [F(y_j - \xi)]\{P_n(\xi)\} \, d\xi \tag{64}$$

and $\{L_{sn}\}$ can be obtained from Eq. (64) by replacing y_j with y_s.

The accuracy of the excessive multiplications of the transfer matrices can be improved by introducing expanded delta matrices.[7,11] An expanded delta transfer matrix $[T^\Delta]$ whose elements consist of all possible subdeterminants of order 2×2 is constructed as

$${}_s^l[T^\Delta]_0^l = [F_s^\Delta][G^\Delta]_j[F^\Delta]_j[G^\Delta]_{j-1} \cdots [F^\Delta]_1[G^\Delta]_0 \tag{65}$$

where

$$[F^\Delta]_j = [B^\Delta][R^\Delta]_j([B]^{-1})^\Delta \tag{66}$$

and the delta matrices, denoted by Δ, are of order 6×6. Thus, using subdeterminants, terms identically equal to zero are evaluated early, i.e., avoiding numbers which are the small difference of two other large numbers. In addition, the other terms are calculated with much greater accuracy.

The solution for the state vector $\{\boldsymbol{Z}_n\}_0^l$ in Eq. (61) can be obtained by applying boundary conditions at $y = 0$ and $y = L_y$. In this approach, boundaries corresponding to simple, fixed, free, or elastic supports can be considered (not necessary the same at both ends). Then, after the solution for the state vector $\{Z_n\}_0^l$ is known, the response state vector $\{\boldsymbol{Z}_n\}_s^l$ can be obtained from Eq. (61).[8] Finally, the response state vector in terms of displacement, slope moment, and shear can be obtained at any arbitrary location on the stiffened panel from[7-9]

$$\{W(x,\omega)\}_s^l = \sum_{n=1}^{\infty} \{Z_n\}_s^l X_n(x) \tag{67}$$

The first element of the response state vector $\{\boldsymbol{W}(x,\omega)\}_s^l$ from Eq. (66) is the displacement component $\bar{w}_s(x,\omega)$ at point (x,y_s). Utilizing the theory of random processes, the response spectral densities corresponding to the four elements in the state vector can be obtained from Eq. (67). For example, the deflection response spectral density at location (x,y_s) can be calculated from[7-9]

$$S^s(x,\omega) = \sum_{n=1}^{\infty} \sum_{m=1}^{\infty} S_{\delta_n\delta_m}^s(\omega) X_n(x) X_m(x) \tag{68}$$

where $S_{\delta_n\delta_m}^s(\omega)$ is the cross spectral density of the amplitude δ_n^s determined from Eq. (61).

Numerical Results

For the calculation of the displacement response and the examination of the importance of the moisture of the stiffened orthotropic panel shown in Fig. 1, simplified versions were chosen for this study. Numerical results were obtained for the stiffened structure shown in Fig. 3. The stiffened panel is composed of three equal bays. Two stiffeners are located at

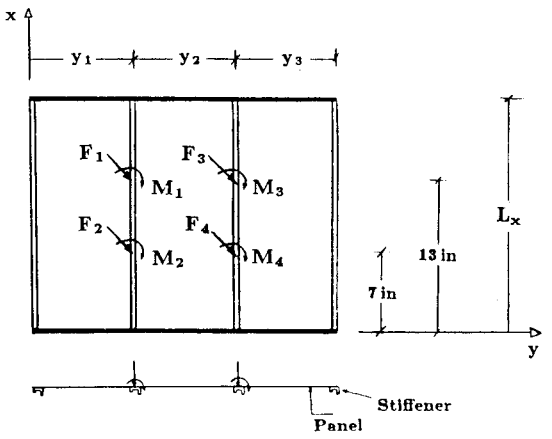

Fig. 3 A three-bay stiffened panel.

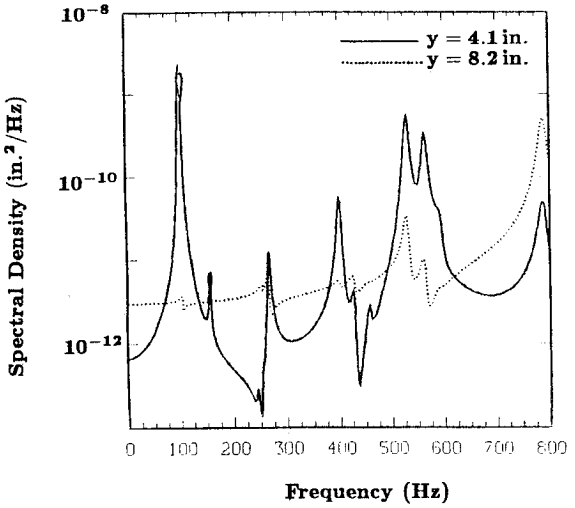

Fig. 4 Deflection response spectral densities to point forces for an orthotropic panel.

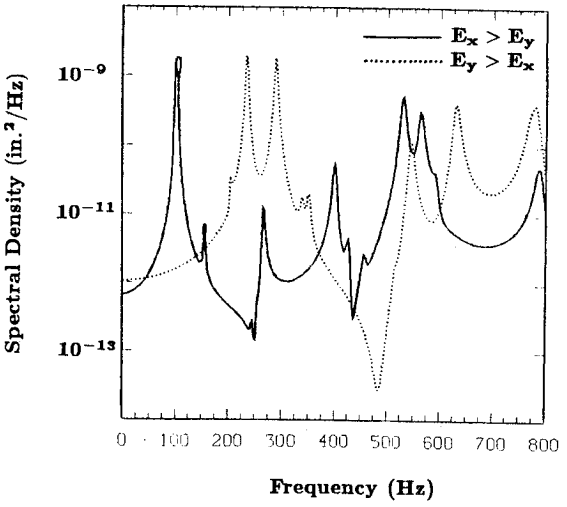

Fig. 5 Deflection response spectral densities for different orientation of the orthotropic material.

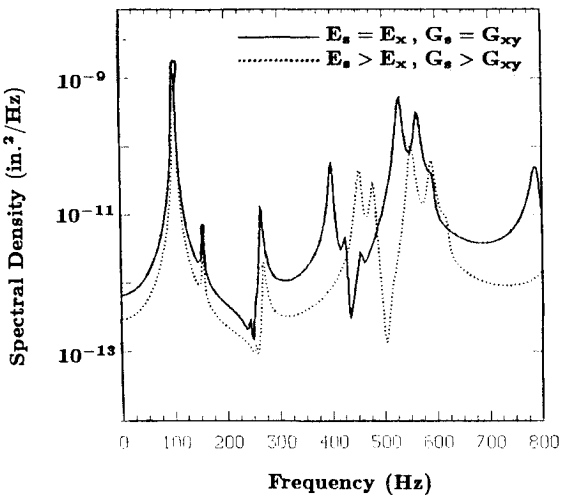

Fig. 6 Deflection response spectral densities for different rigidity of the stiffeners.

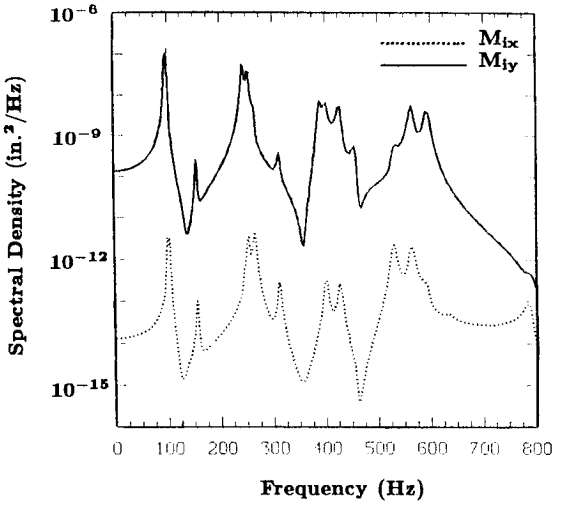

Fig. 7 Deflection response spectral densities to point couples M_{ix} and M_{iy}.

the boundaries, and others are placed at a distance $y_1 = y_2 = y_3 = 8.2$ in. (see Fig. 3). The panel has free boundary conditions at $y = 0, L_y$ (the ends are supported by the end stiffeners). Also, the length of the panel in the x direction is $L_x = 20$ in., and the thickness $h = 0.06$ in. The elastic moduli for the orthotropic panel are assumed to be constant and as follows: $E_x = 2.0 \times 10^7$ psi, $G_{xy} = 0.73 \times 10^6$ psi, $E_y = 1.55 \times 10^6$ psi, the mass density $\rho = 1.373 \times 10^{-4}$ lb · s^2/in.^{4}, the Poisson's ratio $v_{xy} = 0.3$, the hygrothermal coefficients $\beta_x = 0$, $\beta_y = 4.1 \times 10^{-3}$/wt%. The physical parameters for the stiffeners are cross-sectional area $A = 0.2302$ in.^{2}, warping constant $C_{ws} = 0.01649$ in.^{6}, torsion constant $C = 2.263 \times 10^{-4}$ in.^{4}, moments of inertia $I_\eta = 0.122$ in.^{4}, $I_{\eta\zeta} = 0.0$, $I_\zeta = 0.083$ in.^{4}, $J_s = 0.254$ in.^{4}, shear center distances $c_y = 0.0$, $c_z = 0.802$ in., $s_z = 0.082$ in. The elastic constants for the stiffeners are $E_s = 2 \times 10^7$ psi, $G_s = 0.73 \times 10^6$ psi, the mass density $\rho_s = 1.373 \times 10^{-4}$ lb · s^2/in.^{4}, and the Poisson's ratio $v_s = 0.3$.

Damping in the skin-stringer structure is introduced by replacing E_x, E_y, G_{xy}, E_s, and G_s, by $E_x(1 + ig_x)$, $E_y(1 + ig_y)$, $G_{xy}(1 + ig_{xy})$, $E_s(1 + ig_s)$, $G_s(1 + ig_s)$, respectively, where g_x, g_y, g_{xy}, g_s are the loss factors. Numerical results were obtained for $g_x = g_y = g_{xy} = g_s = 0.02$ (damping values are the same for the stiffeners and the panels). The forcing function has the simple form of point forces F_i or point couples M_{ix} or M_{iy} applied on the stiffeners as shown in Fig. 3. The four point forces are assumed to be characterized by truncated Gaussian white noise spectral densities:

$$S_{F_i}(f) = \begin{cases} 0.00084 \text{ lb}^2/\text{Hz} & 0 \leqslant f \leqslant f_u \\ 0 & \text{otherwise} \end{cases} \tag{69}$$

$$S_{M_i}(f) = \begin{cases} 0.00084 \text{ (lb-in.)}^2/\text{Hz} & 0 \leqslant f \leqslant f_u \\ 0 & \text{otherwise} \end{cases} \tag{70}$$

where f is the frequency in Hz, $i = 1,2,3,4$; M_i is either M_{ix} or M_{iy}; and f_u is the upper cutoff frequency. The upper cutoff frequency was taken as $f_u = 800$ Hz. These point loads are located at the positions as indicated in Fig. 3.

Deflection response spectral densities of the orthotropic panel were obtained for different locations. The panel deflection response shown in Fig. 4 is calculated at $x = 5$ in., $y = 4.1$ in., and $y = 8.2$ in. The first point is located at the middle of the bottom half of the first bay, and the second point is at the middle of the half (one-fourth) of the stiffener. The panel is subjected to four equal point forces. Structural modes are excited with different intensity depending on the location. This is critical when sensitive equipment is to be put in different locations. The results presented in Fig. 4 are for the case when the strongest direction of the orthotropic material of the panels is parallel to the stiffeners. In Fig. 5 a comparison between an orthotropic material having stiffer properties in the x direction (i.e., $E_x > E_y$), and an or-

thotropic material having stiffer properties in the y direction (i.e., $E_y > E_x$) is offered. The elastic constants are the same with the exception of the $E_y > E_x$ case, where the orthotropic material is turned 90 deg. The deflection is calculated at the middle of the bottom half of the first bay (i.e., $x = 5$ in. and $y = 4.1$ in.). Depending on the value of frequency, significant differences in response values are obtained. It is difficult to have a general conclusion about the overall displacement (root mean square displacement) because different modes excited more in different locations.

The effect of changing the stiffness of the stiffeners was also studied. In the preceding cases, it was assumed that $E_s = E_x = 2 \times 10^6$ psi and $G_s = G_{xy}$. In Fig. 6 a comparison between the case when $E_s = E_x$, $G_s = G_{xy}$ and the case when $E_s > E_x$, $G_s > G_{xy}$ is presented. For the second case, $E_s = 3 \times 10^7$ psi and $G_s = 1 \times 10^6$ psi. The structural modes which depend strongly on the location and the panel properties are unchanged. However, all the other modes are moved to higher frequencies, as expected. The overall response, for this example, seems significantly lower when the stiffness of the stiffeners is increased.

Spectral densities were also obtained to point couples as shown in Fig. 3. The effect of direction of the input point couple action is illustrated in Fig. 7. The response is calculated at $x = 5$ in. and $y = 6.1$ in. The dashed line corresponds to M_{ix} input (bending effect on the stiffeners) and the solid line to M_{iy} input (twisting effect on the the stiffeners). These results indicate that the deflection response is significantly smaller for bending moment input M_{ix} than for twisting moment input M_{iy}. This is because these stiffeners provide more resistance in bending than in torsion. By tailoring the geometric characteristics, desired response levels can be obtained.

The effect of moisture concentration was also studied. In Fig. 8 moisture is increased from 0 to 0.05 wt%, and 0.08 wt%. The deflection response spectral density is calculated at $x = 5$ in. and $y = 4.1$ in. In general, behavior is similar to the temperature effects. Stiffness is reduced as moisture increases. Thus, resonant frequencies move to lower levels. Similar results are obtained when the stiffness of the stiffeners is increased ($E_s = 3 \times 10^7$ psi, $G_s = 1 \times 10^6$ psi) as shown in Fig. 9. The same observations can be made using different input as in Fig. 10, in which the orthotropic panel is subjected to four equal point couples M_{ix}. The two curves in Figs. 9 and

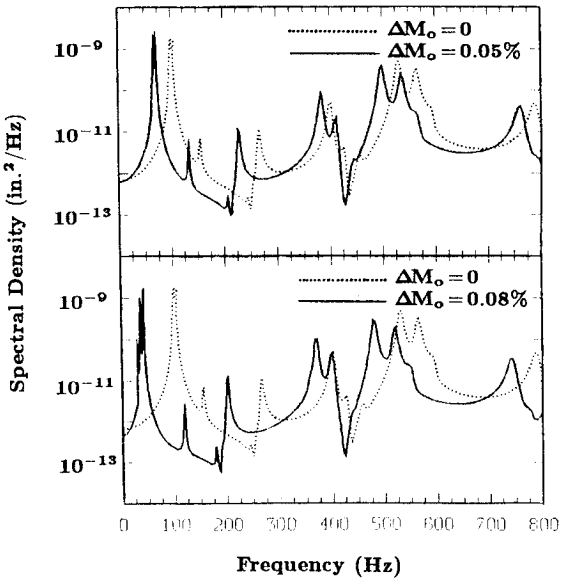

Fig. 8 Deflection response spectral densities for different moisture concentration for an orthotropic panel.

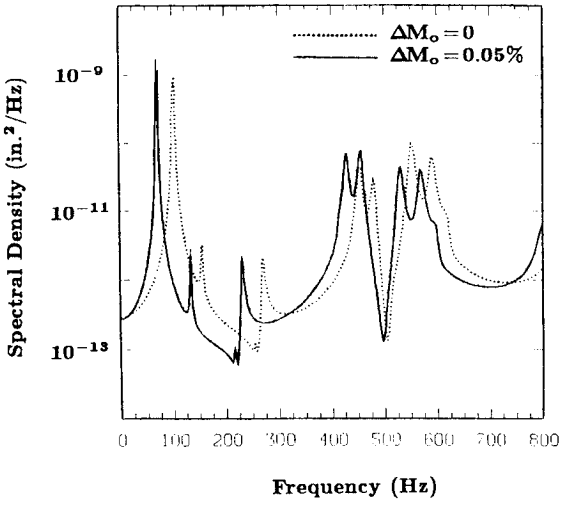

Fig. 9 Deflection response spectral densities for different moisture concentration for an orthotropic panel with increased rigidity of the stiffeners.

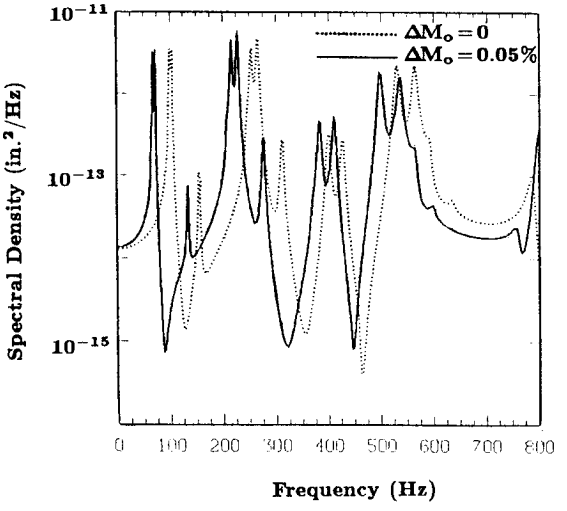

Fig. 10 Deflection response spectral densities for different moisture concentration for an orthotropic panel with point couples M_{ix} input.

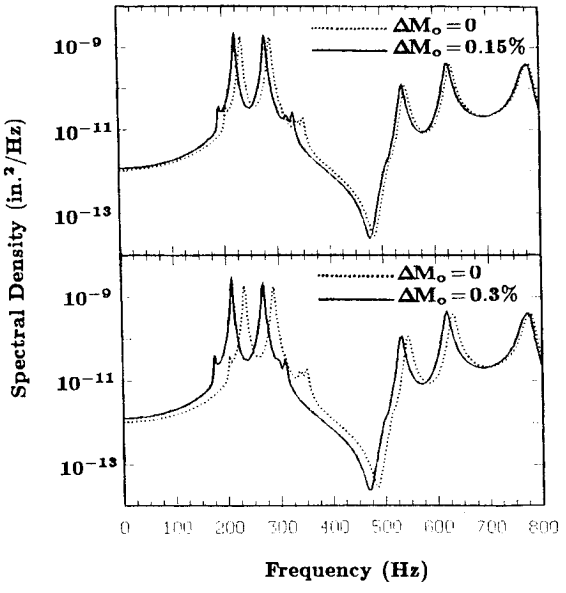

Fig. 11 Deflection response spectral densities for different moisture concentration for an orthotropic panel with $E_y > E_y$.

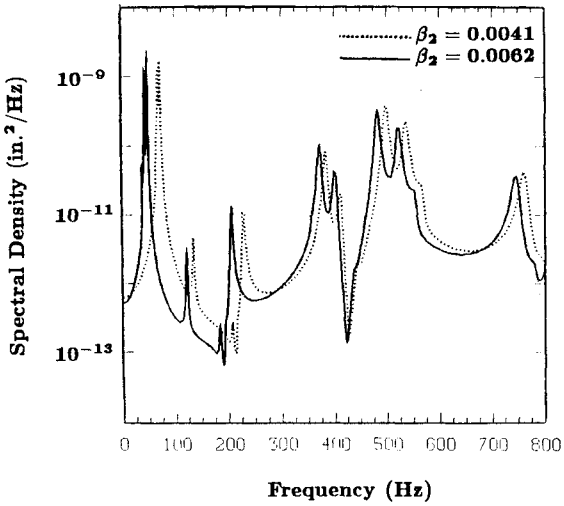

Fig. 12 Deflection response spectral densities for different coefficients of hygroscopic expansion.

10 are for moisture increase 0.05 wt% (solid line) and no moisture (dashed line). However, when the orthotropic material is turned 90 deg, ($E_y > E_x$) the stiffened panel becomes much stronger and changes in moisture do not affect the response as much as before. In Fig. 11 the moisture is increased from 0 to 0.15 wt%, and 0.30 wt%. The results of Fig. 11 demonstrate the same physical significant (increased moisture results in frequencies moving toward lower frequencies) but also the fact that stiffer structures resist much better in moisture effects.

Results are also very sensitive to accurate specifications of the hygroscopic coefficient of the material. A comparison of the sound pressure levels for different coefficients of hygroscopic expansion $\beta_2 = 4.1 \times 10^{-3}$ wt% and $\beta_2 = 6.2 \times 10^{-3}$ wt% is given in Fig. 12.

Conclusions

An analytical method based on transfer matrices has been developed for analyzing the dynamic response of a stiffened orthotropic panel including moisture effects (the effect of temperature was not examined). The formulation can be applied to a variety of discretely stiffened orthotropic and isotropic structures. In addition, it has been shown that structural response is sensitive to the dynamic characteristics of the skin-stiffener structure and to changes in moisture concentrations. The orthotropic stiffened panel response is strongly dependent on the location, the angle of orientation of the orthotropic material, the rigidity of the stiffeners, and the forcing function. It was found that moisture effects on panel response are similar to thermal effects. Resonances corresponding to structural modes of the stiffened panel move to lower frequencies, as the stiffness reduces. Stiffer structures resist in moisture effects better. Dynamic response is very sensitive to the physical constants of the stiffened sidewall. Thus, the coefficient of hygrothermal expansion should be precisely identified.

The results indicate that moisture effects are very important in predicting deflections and transmitted noise. Therefore, these effects must be considered in the design of orthotropic airframe structures, and by tailoring the geometric and material characteristics of structural components vibration levels can be reduced.

Acknowledgment

Constantinos Lyrintzis was supported in part by a grant from the San Diego State University Foundation.

References

[1]Williams, R. M., "National Aero-space Plane: Technology for America's Future," *Aerospace America*, Vol. 108, Nov. 1986.

[2]Davis, G. W., and Sakada, I. F., "Design Considerations for Composite Fuselage Structure of Commercial Transport Aircraft," NASA CR-159296, March 1981.

[3]Mixson, J. S., and Wilby, J. F., "Airplane Interior Noise: A Status Review," AIAA Paper 87-2659, Oct. 1987.

[4]Bofilios, D. A., and Vaicaitis, R., "Response of Double Wall Composite Shells to Random Point Loads," *Journal of Aircraft*, Vol. 24, No. 4, 1987, pp. 268–273.

[5]Vaicaitis, R., and Bofilios, D. A., "Noise Transmission of Double Wall Composite Shells," AIAA Paper 86-1937, July 1986.

[6]Lin, Y. K., and Donaldson, B. K., "A Brief Survey of Transfer Matrix Techniques with Special Reference to Aircraft Panels," *Journal of Sound and Vibration*, Vol. 10, No. 1, 1969, 103–143.

[7]Lyrintzis, C. S., "Response of Discretely Stiffened Structures and Transmission of Structure-borne Noise," Doctoral Thesis, Dept. of Civil Engineering and Engineering Mechanics, Columbia Univ., New York, 1987.

[8]Vaicaitis, R., and Lyrintzis, C. S., "Response of Discretely Stiffened Structures," AIAA Paper 87-0914, April 1987.

[9]Lyrintzis, C. S., and Vaicaitis, R., "Structure-borne Noise Generation and Transmission," *Journal of Probabilistic Engineering Mechanics*, Vol. 2, No. 3, Sept. 1987, pp. 114–120.

[10]Vaicaitis, R., and Choi, S. T., "Response of Stiffened Panels for Applications to Acoustic Fatigue," AIAA Paper 87-2711, Oct. 1987.

[11]Lyrintzis, C., and Vaicaitis, R., "Random Response and Noise Transmission of Discretely Stiffened Composite Panels," *Journal of Aircraft* (to be published).

[12]Vinson, J. R., and Sierakowski, R. L., *The Behavior of Structures Composed of Composite Materials*, Kluwer Publishers, Hingham, MA, 1986.

[13]Pipes, R. B., Vinson, J. R., and Chou, T. W., "On the Hygrothermal Response of Laminated Composite Systems," *Journal of Composite Materials*, Vol. 10, April 1976, pp. 129–148.

[14]Kim, R. Y., and Whitney, J. M., "Effect of Temperature and Moisture on Pin Bearing Strength of Composite Laminates," *Journal of Composite Materials*, Vol. 10, April 1976, pp. 149–155.

[15]Flaggs, D. L., and Vinson, J. R., "Hygrothermal Effects on the Buckling of Laminated Composite Plates," *Journal of Fibre Science and Technology*, Vol. 11, April 1978, pp. 353–365.

[16]Soovere, J., "The Effect of Acoustic/Thermal Environments on Advanced Composite Fuselage Panels," *Journal of Aircraft*, Vol. 10, No. 4, 1985, pp. 257–263.

[17]Timoshenko, S. P., and Goodier, J. N., *Theory of Elasticity*, McGraw-Hill, New York, 1970.

[18]Timoshenko, S. P., and Woinowsky-Krieger, S., *Theory of Plates and Shells*, McGraw-Hill, New York, 1959.

[19]Boley, B. B., and Weiner, J. H., *Theory of Thermal Stresses*, Wiley, New York, 1960.

[20]Friberg, P. O., "Coupled Vibrations of Beams—An Exact Dynamic Element Stiffness Matrix," *International Journal for Numerical Methods in Engineering*, Vol. 19, 1983, pp. 479–493.